PHYSICAL REVIEW A VOLUME 14, NUMBER 4 OCTOBER 1976

Double optical resonance*

R. M. Whitley and C. R. Stroud, Jr.
The Institute of Optics, University of Rochester, Rochester, New York 14627
(Received 18 February 1976)

A complete and detailed treatment of a three-level atom interacting with two near-resonant monochromatic fields is presented. It is assumed that the only damping mechanism is radiative damping, and that the atoms all have the same resonance frequencies, as is the case in an atomic beam. Detailed analytic solutions as well as numerical examples are determined from quantum-electrodynamic equations of motion. In addition, approximation techniques are presented which allow one to get accurate quantitative predictions for strong applied fields from simple rate-equation-like arguments. Absorption and emission spectra are determined, as are the transient and steady-state response of the atom. Two of the more interesting predictions are an emission spectrum containing up to seven components and a prediction of steady-state populations larger than 0.5 in the second excited state.

I. INTRODUCTION

Double resonance using a combination of a resonance lamp and a microwave field has played a central role in optical pumping and high-resolution spectroscopy experiments for the past 25 years.[1] Double optical resonance was also possible using a monochromator and a discharge lamp to obtain the second optical field. This technique was not much used because of two inherent limitations. First, the weak, incoherent light sources did not excite the atoms sufficiently to produce an appreciable population in the second excited state. Beyond that the light source was neither tunable nor monochromatic, so that it did not allow scanning of a high-resolution absorption spectrum.

The recent development of extremely monochromatic, yet tunable, dye lasers[2] has overcome both of these limitations and has made double optical resonance a practical laboratory tool. A few experiments have actually been carried out.[3-6] The further exploitation of this technique seems particularly promising, because of the number of unique capabilities which it offers. In the first place, it allows extremely-high-precision spectroscopy to be carried out on excited states not connected to the ground state by electric dipole transitions.[3-5] Beyond this conventional spectroscopy, it allows one to carry out carefully controlled experiments in which there is competition between spontaneous and stimulated processes. This is the type of experiment which has been the basis of a number of recent tests of the relative merit of quantum electrodynamics (QED) and semiclassical radiation theory.[7] Finally, double optical resonance has been the technique of several proposed methods of laser isotope separation. It is useful in this context for at least two reasons. It produces a large population in a high excited state, which is desirable for either ionization or chemical scavenging separation techniques. Also, if the two optical fields are colinear but oppositely directed, then the Doppler shifts in the two interactions will tend to cancel and atoms will be excited throughout an entire inhomogeneously broadened line.

The interaction of a three-level system with two resonant fields has been extensively discussed in the literature.[8-11] But before the development of dye lasers, the only atomic transitions for which strong resonant fields were readily available were the lasing transitions themselves. The early papers reflected this experimental situation by considering the three-level atoms as comprising the lasing medium. Here, the main effects on the atomic state were due to the incoherent pumping process, transitions (because of atomic collisions) to states outside the resonant three-level system, and the coherent pumping by the laser fields. Radiative decay within the three-level system was a small effect and was neglected in theoretical treatments. Several interesting features for such a system were predicted and observed. Two examples are anisotropic fine structure in the Doppler-broadened emission profile and simultaneous gain and absorption in two different regions of the same Doppler-broadened line. These effects are intimately related to hole burning[12] and the Lamb dip.[13]

The development of dye lasers greatly increased the number of three-level systems which could be investigated by making them independent of the lasing medium. A number of absorption spectra measurements have been made, generally with atoms in a gas cell.[3,4] This required some modification of the previous theoretical treatments. The incoherent, steady-state pumping mechanism for the two excited states could be ignored. The

applied fields could be considered many Doppler widths away from the respective atomic transition frequencies. However, the atomic lines were still considered to be inhomogeneously (Doppler) broadened. Also, collisions are usually the major damping mechanism in gas cells, and the decay terms in the atomic equations of motion were chosen to reflect this situation. As a result the natural radiative lifetimes of the excited states still did not appear in these theories. Power-dependent line shifts and linewidths were predicted for the absorption spectra.[14,15] The possibility of self-induced transparency[6] and self-induced adiabatic rapid passage[16] in such three-level systems has also been discussed.

With resonance experiments now being done on atomic beams,[5,7] theoretical attention is returning to the problem where the only excitation mechanism is the external field, and the only damping present is natural radiative decay. This is the situation that will be described in the present paper, which limits itself to describing a homogeneously broadened atomic system with only radiative damping, such as in a well-collimated atomic-beam experiment. Decay out of the three-level system is not permitted. The applied fields are assumed to have constant intensity after the time $t=0$ when they are turned on. The equations of motion are derived using QED rather than semiclassical theory, which has been used in most of the previous treatments of double resonance. This approach makes use of some recent developments[17] in Heisenberg-picture QED which allow one to derive these equations in a direct and elegant manner. In general, the QED derivation will determine the damping terms entering into the equations of motion and may give terms [e.g., those involving the generalized decay constants of (3.6)] which have not been included in the phenomenological damping of semiclassical theories. However, for the problem considered in this paper, the single-time-operator expectation-value equations do reduce to a form identical to the expected semiclassical Bloch-type equations. The derivation of equations of motion for two-time correlation functions, which are used to find the spectrum of the scattered light, does, of course, require a QED treatment. We develop complete dynamic solutions of the equations and find that the system evolves into a steady-state condition which exhibits a number of interesting features which have not been previously discussed.

In Sec. II we define our notation and discuss some of the approximations made. In Sec. III we develop the basic operator equations of motion and put them into proper form for solution. In Sec. IV we obtain solutions for the dynamics of the dipole moments and the populations of the atomic levels. We discuss the dependence of the steady-state population distribution upon the intensities of the applied fields and present a situation in which the average population in the highest atomic state exceeds 50%. Absorption spectra are described under various conditions. In Sec. V we discuss the equations of motion for two-time-operator products and give their solutions. This allows us to describe the spectrum of the scattered radiation, including the resonant Stark effect. Section VI is devoted to an approximation scheme which provides a straightforward interpretation of some features of our solutions. Basically, the resonant interaction of the atom with the applied field modes is treated by finding the lattice of dressed states of this system. Spontaneous emission is then introduced with an appropriate form of rate equations. Expressions for the atomic population distribution and for the power in the sidebands of the emission spectrum are found and compared with the QED predictions. In Sec. VII we summarize our results. Finally, analytic forms of the steady-state solutions for the dipole moments and atomic populations are given in an appendix.

II. NOTATION AND DESCRIPTION OF THE ATOM-FIELD SYSTEM

Consider the situation illustrated in Fig. 1. A three-level atom has energy levels $E_1<E_2<E_3$, corresponding to the three states $|1\rangle$, $|2\rangle$, $|3\rangle$. It is interacting with an electromagnetic field which initially has only two modes populated. We shall assume that these incident fields are describable by coherent states, although the assumption of Fock states leads to equivalent equations. The frequencies ω_a and ω_b of these modes are near-resonant with the atom's transition frequencies, so that

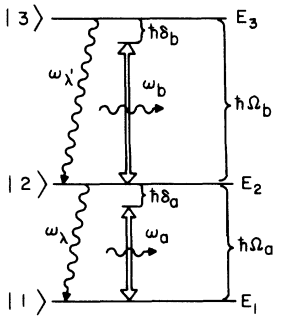

FIG. 1. Three-level atom interacting with the two monochromatic applied fields.

$$\hbar\omega_a \simeq E_2 - E_1 \equiv \hbar\Omega_a, \tag{2.1a}$$

$$\hbar\omega_b \simeq E_3 - E_2 \equiv \hbar\Omega_b. \tag{2.1b}$$

The detunings of the applied fields from exact resonance are defined by

$$\delta_a \equiv \Omega_a - \omega_a, \tag{2.2a}$$

$$\delta_b \equiv \Omega_b - \omega_b. \tag{2.2b}$$

An atomic operator will be denoted by a subscripted σ,

$$\sigma_{ij} = |i\rangle\langle j|, \quad i,j = 1,2,3. \tag{2.3}$$

The atom interacts not only with the incident field modes, but with all modes λ, where λ has four components and specifies the wave-vector and polarization indices. The annihilation and creation operators for the mode λ are c_λ and $c_\lambda^\dagger$. The initially occupied mode of frequency ω_a is denoted by $\lambda = \alpha$, the one of frequency ω_b by $\lambda = \beta$.

The total system is described by a Hamiltonian H consisting of an atomic part, a field part, and an interaction part:

$$H = H_A + H_F + H_I. \tag{2.4}$$

The atomic part satisfies the eigenvector equation

$$H_A|m\rangle = E_m|m\rangle, \quad m = 1,2,3. \tag{2.5}$$

The field part of the Hamiltonian is the usual expression

$$H_F = \hbar\sum_\lambda \omega_\lambda c_\lambda^\dagger c_\lambda. \tag{2.6}$$

The interaction part of the Hamiltonian can be written in the dipole and rotating-wave approximations in the form

$$H_I = \hbar\sum_\lambda (g_a^\lambda \sigma_{21} c_\lambda + g_a^{\lambda *} c_\lambda^\dagger \sigma_{12} + g_b^\lambda \sigma_{32} c_\lambda + g_b^{\lambda *} c_\lambda^\dagger \sigma_{23}). \tag{2.7}$$

The factors g_a^λ and g_b^λ are the usual coupling constants

$$g_a^\lambda = -ie\hat{\epsilon}_\lambda \cdot \vec{d}_a (2\pi\omega_\lambda/\hbar V)^{1/2} \tag{2.8a}$$

$$g_b^\lambda = -ie\hat{\epsilon}_\lambda \cdot \vec{d}_b (2\pi\omega_\lambda/\hbar V)^{1/2} \tag{2.8b}$$

where $\hat{\epsilon}_\lambda$ is the polarization vector of the λ mode, $\vec{d}_a = \langle 2|\vec{r}|1\rangle$, $\vec{d}_b = \langle 3|\vec{r}|2\rangle$, and V is the quantization volume. We have explicitly taken $\langle 3|\vec{r}|1\rangle$ to be zero. Also, $\hbar|\Omega_a - \Omega_b|$ is assumed to be much greater than the interaction energies or $\hbar$ times the Einstein A coefficients of the atomic levels, so that there is no difficulty in associating a particular emitted frequency with one or the other of the atomic transitions. This excludes the possibility of equally spaced levels, a situation which is of interest in microwave double resonance, but of less importance for optical double resonance. We have written H_I in a kind of "normal order," with the field annihilation and creation operators placed to the extreme right-hand and left-hand sides, respectively, in each operator product. This is possible since atomic operators always commute with field operators having the same time argument. This ordering leads to some computational simplification,[17] although it is strictly equivalent to any other ordering.[18] Finally, it is well known that in making the rotating-wave approximation, we are throwing away terms which contribute to radiative and Bloch-Siegert-like shifts. For consistency, similar terms (i.e., terms which can be identified as rapidly oscillating) and their contributions to such frequency shifts will be neglected throughout this calculation. Moreover, since our principal interest concerns the effects due to the applied fields, those shifts which occur even in the absence of such applied fields will in general be ignored or assumed to have been incorporated in the atomic transition frequencies.

III. OPERATOR EQUATIONS OF MOTION

The equation of motion for a single time operator $O(t)$ is given by $\dot{O}(t) = (i\hbar)^{-1}[O,H]$. Using the Hamiltonian (2.4), we find that the atom-field system evolves according to the following equations:

$$\dot{\sigma}_{11} = i\sigma_{21}\sum_\lambda g_a^\lambda c_\lambda - i\sum_\lambda g_a^{\lambda *} c_\lambda^\dagger \sigma_{12}, \tag{3.1a}$$

$$\dot{\sigma}_{33} = -i\sigma_{32}\sum_\lambda g_b^\lambda c_\lambda + i\sum_\lambda g_b^{\lambda *} c_\lambda^\dagger \sigma_{23}, \tag{3.1b}$$

$$\dot{\sigma}_{21} = i\Omega_a\sigma_{21} + i\sigma_{31}\sum_\lambda g_b^\lambda c_\lambda - i\sum_\lambda g_a^{\lambda *} c_\lambda^\dagger(\sigma_{22} - \sigma_{11}), \tag{3.1c}$$

$$\dot{\sigma}_{32} = i\Omega_b\sigma_{32} - i\sigma_{31}\sum_\lambda g_a^\lambda c_\lambda - i\sum_\lambda g_b^{\lambda *} c_\lambda^\dagger(\sigma_{33} - \sigma_{22}), \tag{3.1d}$$

$$\dot{\sigma}_{31} = i(\Omega_a + \Omega_b)\sigma_{31} - i\sum_\lambda g_a^{\lambda *} c_\lambda^\dagger \sigma_{32} + i\sum_\lambda g_b^{\lambda *} c_\lambda^\dagger \sigma_{21}, \tag{3.1e}$$

$$\dot{c}_\lambda = -i\omega_\lambda c_\lambda - ig_a^{\lambda *}\sigma_{12} - ig_b^{\lambda *}\sigma_{23}. \tag{3.1f}$$

The field equation (3.1f) can be formally integrated from the initial time $t = 0$ of the interaction, yielding

$$c_\lambda(t) = c(0)e^{-i\omega_\lambda t} - ig_a^{\lambda *}\int_0^t \sigma_{12}(t')e^{-i\omega_\lambda(t-t')}dt' - ig_b^{\lambda *}\int_0^t \sigma_{23}(t')e^{-i\omega_\lambda(t-t')}dt'. \tag{3.2}$$

When expression (3.2) is substituted for the field operators in Eqs. (3.1a)–(3.1e), the atomic operator equations are found to contain only initial-time field operators.

It is customary to treat integrals like those appearing in (3.2) by making the *harmonic approximation,* which assumes the atomic operators evolve as they would in the absence of any coupling to the field:

$$\sigma_{12}(t') = \sigma_{12}(t)e^{i\Omega_a(t-t')},$$
$$\sigma_{23}(t') = \sigma_{23}(t)e^{i\Omega_b(t-t')}.$$

The validity of this approximation is limited to time intervals much shorter than a Rabi period or a natural lifetime. It will be used only when the $\sigma(t')$ appears inside an integral over time and summation over frequency, such as

$$\sum_\lambda |g_a^\lambda|^2 \int_0^T \sigma_{12}(t')e^{-i\omega_\lambda(t-t')}dt' \simeq \sigma_{12}(t)\sum_\lambda |g_a^\lambda|^2 \int_0^T e^{-i(\omega_\lambda-\Omega_a)(t-t')}dt'. \quad (3.3)$$

Here the harmonic approximation is justified, because the sum over all modes will force only those values of t' within a few optical periods of t to make a significant contribution to the integral. When $t=T$, the upper limit on the integral in (3.3), this treatment leads to a decay constant and a frequency shift.[17] We shall ignore this frequency shift, which arises from a principal-part integral and has been discussed in some detail, particularly for the two-level atom.[17-19] Alternatively, one could assume that such shifts have been incorporated into the original definitions of Ω_a and Ω_b.

Using this approach we eliminate the operators evaluated at t' which appeared after substitution of (3.2) into (3.1). The atomic operator equations of motion become

$$\dot\sigma_{11} = 2\Gamma_a\sigma_{22} + i\sigma_{21}\sum_\lambda g_a^\lambda e^{-i\omega_\lambda t}c_\lambda(0) - i\sum_\lambda c_\lambda^\dagger(0)g_a^{\lambda*}e^{i\omega_\lambda t}\sigma_{12}, \quad (3.4a)$$

$$\dot\sigma_{33} = -2\Gamma_b\sigma_{33} - i\sigma_{32}\sum_\lambda g_b^\lambda e^{-i\omega_\lambda t}c_\lambda(0) + i\sum_\lambda c_\lambda^\dagger(0)g_b^{\lambda*}e^{i\omega_\lambda t}\sigma_{23}, \quad (3.4b)$$

$$\dot\sigma_{21} = (i\Omega_a - \Gamma_a)\sigma_{21} + (\Gamma_{ab}^* + \Gamma_{ba})\sigma_{32} + i\sigma_{31}\sum_\lambda g_b^\lambda e^{-i\omega_\lambda t}c_\lambda(0) - i\sum_\lambda c_\lambda^\dagger(0)g_a^{\lambda*}e^{i\omega_\lambda t}(\sigma_{22}-\sigma_{11}), \quad (3.4c)$$

$$\dot\sigma_{32} = (i\Omega_b - \Gamma_a - \Gamma_b)\sigma_{32} - i\sigma_{31}\sum_\lambda g_a^\lambda e^{-i\omega_\lambda t}c_\lambda(0) - i\sum_\lambda c_\lambda^\dagger(0)g_b^{\lambda*}e^{i\omega_\lambda t}(\sigma_{33}-\sigma_{22}), \quad (3.4d)$$

$$\dot\sigma_{31} = (i\Omega_a + i\Omega_b - \Gamma_b)\sigma_{31} - i\sum_\lambda c_\lambda^\dagger(0)g_a^{\lambda*}e^{i\omega_\lambda t}\sigma_{32} + i\sum_\lambda c_\lambda^\dagger(0)g_b^{\lambda*}e^{i\omega_\lambda t}\sigma_{21}, \quad (3.4e)$$

where the decay constants, which are half the usual Einstein A coefficients, are defined by

$$\Gamma_a \equiv \sum_\lambda |g_a^\lambda|^2\pi\delta(\Omega_a-\omega_\lambda), \quad (3.5a)$$

$$\Gamma_b \equiv \sum_\lambda |g_b^\lambda|^2\pi\delta(\Omega_b-\omega_\lambda), \quad (3.5b)$$

and the generalized decay constants[20] are given by

$$\Gamma_{ab} \equiv \sum_\lambda g_a^\lambda g_b^{\lambda*}\pi\delta(\Omega_b-\omega_\lambda), \quad (3.6a)$$

$$\Gamma_{ba} \equiv \sum_\lambda g_b^\lambda g_a^{\lambda*}\pi\delta(\Omega_a-\omega_\lambda). \quad (3.6b)$$

We take the expectation value of Eqs. (3.4) in a product state of a monochromatic coherent state for each of the initially occupied field modes and an arbitrary initial state for the three-level atom. Common oscillations at optical frequencies are removed by transforming to slowly varying operators:

$$\chi_{ii}(t) = \sigma_{ii}(t), \quad \chi_{31}(t) = \sigma_{31}(t)e^{-i(\omega_a+\omega_b)t},$$
$$\chi_{21}(t) = \sigma_{21}(t)e^{-i\omega_a t}, \quad \chi_{32}(t) = \sigma_{32}(t)e^{-i\omega_b t},$$

and similarly for their Hermitian conjugates. The equations for the expectation values are

$$\langle\dot\chi_{11}\rangle = 2\Gamma_a\langle\chi_{22}\rangle + iG_a\langle\chi_{21}\rangle - iG_a^*\langle\chi_{12}\rangle, \quad (3.7a)$$

$$\langle\dot\chi_{33}\rangle = -2\Gamma_b\langle\chi_{33}\rangle - iG_b\langle\chi_{32}\rangle + iG_b^*\langle\chi_{23}\rangle, \quad (3.7b)$$

$$\langle\dot\chi_{21}\rangle = (i\delta_a - \Gamma_a)\langle\chi_{21}\rangle + iG_b\langle\chi_{31}\rangle - iG_a^*\langle\chi_{22}-\chi_{11}\rangle, \quad (3.7c)$$

$$\langle\dot\chi_{32}\rangle = (i\delta_b - \Gamma_a - \Gamma_b)\langle\chi_{32}\rangle - iG_a\langle\chi_{31}\rangle - iG_b^*\langle\chi_{33}-\chi_{22}\rangle, \quad (3.7d)$$

$$\langle\dot\chi_{31}\rangle = (i\delta_a + i\delta_b - \Gamma_b)\langle\chi_{31}\rangle - iG_a^*\langle\chi_{32}\rangle + iG_b^*\langle\chi_{21}\rangle, \quad (3.7e)$$

where

$$G_a \equiv g_a^\alpha\langle c_\alpha(0)\rangle, \quad (3.8a)$$

$$G_b \equiv g_b^\beta\langle c_\beta(0)\rangle. \quad (3.8b)$$

Note that the Γ_{ab}^* and Γ_{ba} terms in the σ_{21} equation no longer appear. If $\vec d_a$ and $\vec d_b$ are orthogonal,

these factors are identically zero. In general the Γ_{ab} and Γ_{ba} are nonzero, but the time dependence of the terms in which they appear (in the slowly varying operator equations) includes an oscillation at the frequency $\omega_a - \omega_b$. Because $\hbar|\omega_a - \omega_b|$ has been assumed to be much larger than either the interaction energies $\hbar|G_a|$ and $\hbar|G_b|$ or $\hbar\Gamma_a$ and $\hbar\Gamma_b$, such terms are rapidly oscillating and have been neglected. This could not be done for equally spaced atomic levels, unless $\vec{d}_a \cdot \vec{d}_b = 0$.

We mention here that the assumption that the two monochromatic applied fields are coherent states is not strictly necessary. One can alternatively go to the thermodynamic limit, where the quantization volume V and also the photon numbers $\langle n_\alpha \rangle$ and $\langle n_\beta \rangle$ become infinite, but in such a way that the photon densities $\langle n_\alpha \rangle / V$ and $\langle n_\beta \rangle / V$ approach finite values. In this case equations equivalent to (3.7) can be derived, independent of the specific form of the states of the two initially occupied modes. By equivalent, we mean that the predicted response of the atomic system (e.g., its emission spectrum and the time development of the population distribution) as a function of the intensities and detunings of the incident fields is identical.

Although these equations have been derived using QED, they are identical to the Bloch-type equations one expects for this problem. For this reason they are similar to equations previously found by other investigators[8-11,14,15] when the applied fields were assumed to be classical and damping was added phenomenologically. Because those treatments describe atoms in a gas, the main difference between their equations and ours is in the decay terms. Their equations describe a situation where the relaxation between the atomic levels $|1\rangle$, $|2\rangle$, and $|3\rangle$ is slow compared to the decay from these states to levels outside the resonant system. This is the opposite of the situation described in this paper. A direct comparison shows that the decay terms in the off-diagonal matrix element equations in Refs. 8–11 and 15 can be chosen to make those equations equivalent to our equations (3.7c)–(3.7e). However, the equations for the level populations found in those papers and in the paper by Brewer and Hahn[14] differ from ours, even when their incoherent "background" pumping terms are set equal to zero. This is because their phenomenological decay matrix was chosen to be diagonal, so that an excited state can decay only out of the three-level system, and not to another state within it. In contrast, under our equations the equality

$$\langle \chi_{11} \rangle + \langle \chi_{22} \rangle + \langle \chi_{33} \rangle = 1 \tag{3.9}$$

holds for all time.

If we now add to Eqs. (3.7) the equations for $\langle \chi_{22} \rangle$, $\langle \chi_{12} \rangle$, $\langle \chi_{23} \rangle$, and $\langle \chi_{13} \rangle$, we find a closed set of nine equations. They are particularly simple because they are linear coupled differential equations with constant coefficients. In matrix notation they can be simply written

$$\frac{d}{dt} V(t) = A V(t) . \tag{3.10}$$

$V(t)$ is a 9×1 column vector. We take its elements to be $V_1 = \langle \chi_{33} \rangle$, $V_2 = \langle \chi_{32} \rangle$, $V_3 = \langle \chi_{31} \rangle$, $V_4 = \langle \chi_{21} \rangle$, $V_5 = \langle \chi_{11} \rangle$, $V_6 = \langle \chi_{12} \rangle$, $V_7 = \langle \chi_{13} \rangle$, $V_8 = \langle \chi_{23} \rangle$, and $V_9 = \langle \chi_{22} \rangle$. With this choice of ordering the 9×9 matrix A becomes

$$A = \begin{bmatrix}
-2\Gamma_b & -iG_b & 0 & 0 & 0 & 0 & 0 & iG_b^* & 0 \\
-iG_b^* & i\delta_b - \Gamma_a - \Gamma_b & -iG_a & 0 & 0 & 0 & 0 & 0 & iG_b^* \\
0 & -iG_a^* & i\delta_a + i\delta_b - \Gamma_b & iG_b^* & 0 & 0 & 0 & 0 & 0 \\
0 & 0 & iG_b & i\delta_a - \Gamma_a & iG_a^* & 0 & 0 & 0 & -iG_a^* \\
0 & 0 & 0 & iG_a & 0 & -iG_a^* & 0 & 0 & 2\Gamma_a \\
0 & 0 & 0 & 0 & -iG_a & -i\delta_a - \Gamma_a & -iG_b^* & 0 & iG_a \\
0 & 0 & 0 & 0 & 0 & -iG_b & -i\delta_a - i\delta_b - \Gamma_b & iG_a & 0 \\
iG_b & 0 & 0 & 0 & 0 & 0 & iG_a^* & -i\delta_b - \Gamma_a - \Gamma_b & -iG_b \\
2\Gamma_b & iG_b & 0 & -iG_a & 0 & iG_a^* & 0 & -iG_b^* & -2\Gamma_a
\end{bmatrix} . \tag{3.11}$$

IV. SOLUTIONS OF THE EQUATIONS OF MOTION

The solution of (3.10) is formally given by

$$V_i(t) = \sum_{m=1}^{9} \sum_{j=1}^{9} v_i(m) w_j(m) V_j(0) e^{s_m t} . \tag{4.1}$$

Here s_m is one of the nine eigenvalues of A. The 9×1 column vectors $v(m)$ and $w(m)$ are, respectively, the eigenvector and reciprocal eigenvector associated with s_m. These quantities are readily evaluated numerically by computer, giving us

complete dynamical solutions for the expectation value of any of the nine atomic operators. These solutions are a function of the six parameters of the theory: the two decay constants, Γ_a and Γ_b; the detuning of each of the modes from resonance, δ_a and δ_b; and the interaction energy of each transition, $\hbar|G_a|$ and $\hbar|G_b|$.

For the general situation in which both interaction energies and decay constants are nonzero, one eigenvalue will be zero. For convenience we order them so that it is the first eigenvalue: $s_1 = 0$. The corresponding reciprocal eigenvector $w(1)$ can be chosen so that its only nonzero elements, $w_1(1) = w_5(1) = w_9(1)$, are equal to unity. (Note that this represents the combination of operators which form the identity.) All of the other eigenvalues have a negative real part. Therefore in the long-time limit all nine expectation values $V_i(t)$ assume values which are independent of time. These steady-state values are independent of the atom's initial condition, as one can see from (4.1). In the long-time limit it simplifies to

$$\lim_{t\to\infty} V_i(t) = \sum_j v_i(1) w_j(1) V_j(0) = v_i(1). \tag{4.2}$$

Rather than attempt an exhaustive description of the solutions (4.1) and (4.2), we shall limit ourselves to a detailed discussion of certain interesting specific cases. However, general analytic forms of the steady-state solutions (4.2) are given in the Appendix.

One of the most interesting questions which our theory can answer concerns the steady-state population distribution. How much population can be put into the middle and highest atomic states? We shall be interested in comparing our results to those given by rate equations for the atomic-state populations. From such a rate-equation analysis one finds that the inequality

$$\langle\sigma_{11}\rangle > \langle\sigma_{22}\rangle > \langle\sigma_{33}\rangle \tag{4.3}$$

must always hold. In the limit of the stimulated transition rates becoming very much larger than the spontaneous decay rates, the population of each state approaches $\frac{1}{3}$. The predictions of our theory are qualitatively different from (4.3) and are somewhat surprising. It is possible to have $\langle\sigma_{33}\rangle > \langle\sigma_{22}\rangle$, or $\langle\sigma_{22}\rangle > \langle\sigma_{11}\rangle$, though both conditions cannot be simultaneously satisfied.

We have first considered a three-level atom with decay rates $\Gamma_a = 10$ and $\Gamma_b = 3.33$. It should be noted that for compactness we have omitted the units of our parameters G_a, G_b, Γ_a, Γ_b, δ_a, and δ_b. By inspection of Eqs. (3.7) one knows the units must have dimensions of rad/sec. But the magnitude of the units is arbitrary, since multiplying all frequencies by a scale factor leaves the results unchanged. This scale factor can be chosen to approximate various particular systems. For example, if the units are considered to be 3.1×10^6 rad/sec, then $\Gamma_a = 10$ implies that the first excited state has a lifetime $\tau_a = 1/(2\Gamma_a) = 16.1$ nsec, the lifetime of the $3p$ levels in sodium. Taking $|G_a| = 50$ would then imply that the laser light at the lower transition frequency is strong enough so that when it is exactly resonant it causes the atomic population to oscillate between the ground state and the first excited state with a Rabi frequency $\Omega_R = 2|G_a|$ and a Rabi period $T_R = 2\pi/\Omega_R = 20$ nsec. The critical intensity, which is defined as giving a Rabi frequency of half the Einstein A coefficient, is about 5 mW/cm^2 for the $3s$-$3p$ transition in sodium.[21] Thus $|G_a| = 50$ is ten times the critical field and corresponds to an intensity of about 500 mW/cm^2 at one of the sodium D lines.

Both applied-field modes are exactly resonant ($\delta_a = 0 = \delta_b$) and the interaction energies are taken equal. In Fig. 2(a) we show the steady-state atomic populations as a function of the interaction energy $|G| = |G_a| = |G_b|$. For $|G| \geq 5$, $\langle\sigma_{33}\rangle$ is greater than $\langle\sigma_{22}\rangle$. In fact, $\langle\sigma_{33}\rangle$ becomes significantly greater than $\langle\sigma_{22}\rangle$, since they asymptotically approach the values 0.4 and 0.2, respectively. One sees that already $\langle\sigma_{22}\rangle > 0.19$ and $\langle\sigma_{33}\rangle > 0.36$ for $|G| = 20$.

If we now detune the two applied fields in opposite directions by 200, so that $\delta_a = 200 = -\delta_b$, we find the population distributions shown in Fig. 2(b). For weak fields the excitation is less than when the fields were exactly resonant. For stronger fields, however, the detuning actually increases the population in the upper excited state. In both Fig. 2(a) and 2(b), $\langle\sigma_{33}\rangle \simeq 0.392$ at $|G| = 45$. But with the opposite detunings and $|G| > 53$, $\langle\sigma_{33}\rangle > 0.4$, a value it reaches only asymptotically for exactly resonant fields. For the situation of Fig. 2(b), $\langle\sigma_{33}\rangle$ reaches a maximum value just above 0.406 near $|G| = 80$ and then begins to decrease slightly.

Conditions whereby the lower transition may become inverted are shown in Fig. 3. The decay constant is the same for both excited states, with $\Gamma_a = \Gamma_b = 10$. The exactly resonant applied fields have been chosen so that the interaction energies for the first and second transitions are in a 2:1 ratio, $|G| = |G_a| = 2|G_b|$. Again the atomic-state populations are plotted as a function of $|G|$. Beyond the crossover point at $|G| \simeq 32$ the middle state has a greater population than the ground state. As $|G|$ becomes very large, the populations asymptotically approach the limits

$$\langle\sigma_{11}\rangle = \tfrac{17}{45}, \quad \langle\sigma_{22}\rangle = \tfrac{20}{45}, \quad \langle\sigma_{33}\rangle = \tfrac{8}{45}.$$

We have so far discussed situations when $\langle\sigma_{33}\rangle$

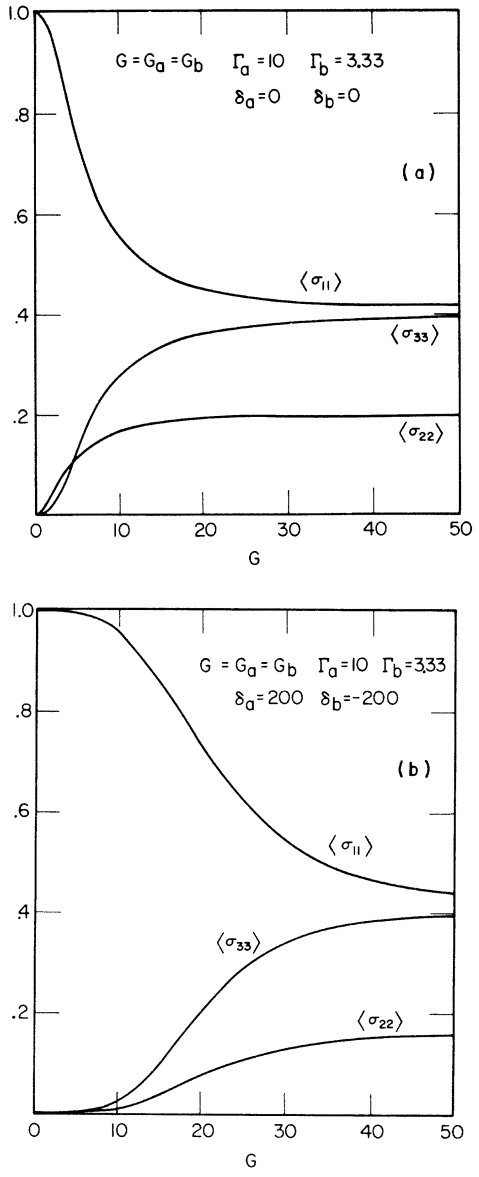

FIG. 2. Steady-state atomic population distribution as a function of the strength of the applied fields, (a) which are exactly resonant (the upper transition becomes inverted), and (b) which have detunings of equal magnitude but opposite sign.

$> \langle\sigma_{22}\rangle$ and where $\langle\sigma_{22}\rangle > \langle\sigma_{11}\rangle$. It is also possible to have $\langle\sigma_{33}\rangle > \langle\sigma_{11}\rangle$. For the parameters $\Gamma_a = 10$, $\Gamma_b = 1$, $\delta_a = 0 = \delta_b$, $|G_a| = 48$, and $|G_b| = 32$, one finds $\langle\sigma_{11}\rangle = 0.326$, $\langle\sigma_{22}\rangle = 0.154$, and $\langle\sigma_{33}\rangle = 0.520$ in the steady state. Not only is the third state's population greater than the ground state's, it is greater than $\frac{1}{2}$! In Sec. VI the conditions for getting a large steady-state population in the upper excited state are discussed in some detail.

The atomic population distributions we have discussed above are interesting not only in their own right but also because of how strongly the rate-equation predictions (4.3) are violated. But upon reflection this disagreement is reasonable. The rate equations assume that the off-diagonal elements of the density matrix are zero or negligible. This is a poor assumption when an applied field is creating a coherent superposition of the atomic states. In the last example above, where $\langle\sigma_{33}\rangle = 0.520$, the steady-state value of $|\langle\chi_{13}\rangle|$ is 0.248, or more than 60% of its maximum possible value of $(\langle\sigma_{11}\rangle\langle\sigma_{33}\rangle)^{1/2}$, which is attained only when the superposition of the states $|1\rangle$ and $|3\rangle$ is a pure state. This will be discussed further in Sec. VI.

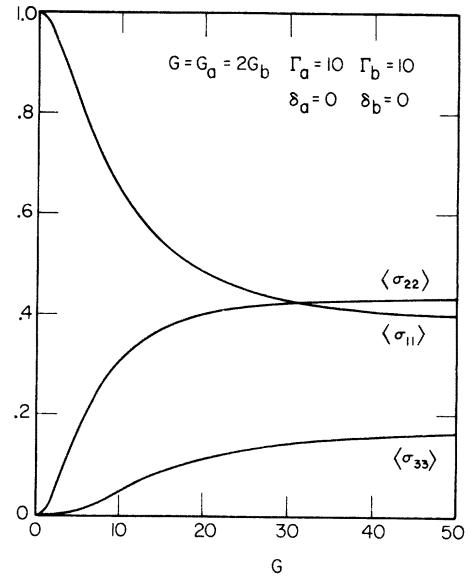

FIG. 3. Population distribution as a function of the applied-field strengths, showing a situation where the lower transition becomes inverted for strong fields.

One of the recent practical uses of double optical resonance has been absorption spectroscopy.[3-5] By tuning one of the applied-field frequencies while simultaneously monitoring the intensity of the fluorescence from the middle or highest states, one can directly measure such quantities as upper excited-state fine structure. Because the fluorescence from the middle and the highest states is proportional to $\Gamma_a\langle\sigma_{22}\rangle$ and $\Gamma_b\langle\sigma_{33}\rangle$, respectively, one can model these experiments by calculating the atomic-state populations as a function of the detuning of one of the fields. We have done this for a three-level atom with $\Gamma_a = 5$ and $\Gamma_b = 2$. The first field mode is held fixed while the frequency of the second field is tuned over the relevant region. We have first treated the situation where both fields are strong, $|G_a| = |G_b| = 30$. The results for detunings of the first applied-field mode of 0, 80, and 800 are shown in Fig. 4. The width of the

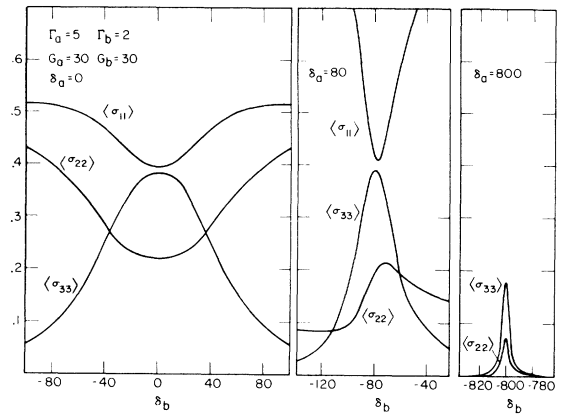

FIG. 4. Absorption spectra for both fields strong, for three different fixed detunings of the field exciting the lower transition.

absorption spectrum for the second transition (curve $\langle\sigma_{33}\rangle$) is strongly dependent upon the detuning of the applied-field modes. For $\delta_a = 0$, the half width at half-maximum (HWHM) is about 50, far greater than the natural width of the first or second transition. This phenomenon is power broadening. A strong field can appreciably excite a transition even when it is somewhat off-resonance.

For $\delta_a = 80$ the peak in the curve $\langle\sigma_{33}\rangle$ has shifted to $\delta_a = -80$. At the point of overall resonance $\delta_a + \delta_b = 0$ the height of the peak, and hence the intensity of the fluorescence, has actually increased slightly to 0.390 from 0.383 for $\delta_a = 0$. The HWHM has decreased significantly, to about 19. The $\langle\sigma_{33}\rangle$ curve is slightly skewed, and the $\langle\sigma_{22}\rangle$ curve peaks at −72 instead of at the overall resonance point.

Finally, Fig. 4 shows than for $\delta_a = 800$, $\langle\sigma_{33}\rangle$ again peaks when $\delta_a + \delta_b = 0$. At the peak the average population in the upper excited state is 0.178, and is 0.072 in the middle state, which also peaks sharply at this point. Though this is lower than the peak populations for smaller field detunings, it still represents a very significant excitation and yields an easily detectable fluorescence signal. The HWHM of both curves is about 2.7, which is one-third greater than the natural width of the upper excited state. It is, however, significantly less than the half-width of the spontaneous emission from the third level, which is the sum of the widths of the first and upper excited states. This means that upper states separated by several natural widths (e.g., about eight here) could be individually resolved in the absorption spectrum when $\delta_a = 800$. This compares to a resolution of only about 120 for $\delta_a = 0$.

The fact that $\langle\sigma_{33}\rangle$ peaks when the overall detuning $\delta_a + \delta_b$ is zero is not a general result for strong fields but rather a consequence of the equal interaction energies. If $|G_a| = 30$ while $|G_b|$ is decreased to 10, then the peak for $\langle\sigma_{33}\rangle$ shifts from −800 to −801. The excited-state populations are down by a factor of 5, and the HWHM for the lower and upper transition absorption curves are 2.1 and 2.4, respectively. The shift and width of this absorption peak in a gas cell have been discussed by Brewer and Hahn[14] [see their equations (40) and (41)].

If the second applied field is a weak "probe" field, the absorption curves differ radically. We have decreased $|G_b|$ to 1 and plotted $\langle\sigma_{33}\rangle$ as a function of δ_b for $\delta_a = 0$, 40, and 80 in Fig. 5. The spectra are now double peaked. For $\delta_a = 0$ the spectrum is a symmetric doublet peaking at roughly ±30. This shape is readily understood in terms of the dressed states of the strongly driven lower transition, which are doublets containing equal amounts of the first and second atomic states.[22] A peak occurs when the second field is resonant with the transition from either of the doublet states to the third atomic state. As δ_a increases, the upper dressed state of the doublet contains more of the second atomic state, and the lower dressed state contains more of the ground state. Thus for large detunings δ_a, the third atomic state is connected by a much larger dipole moment to the upper dressed state than to the lower. Nevertheless, the last two curves of Fig. 5 reach their maximum values when the probe field is tuned to the lower dressed state. The much larger population in this state more than compensates for the smaller dipole moment between it and the third atomic state.

For the absorption spectra described above, δ_b was varied while δ_a remained fixed. One could instead vary the lower transition field frequency while holding δ_b fixed. For this second type of

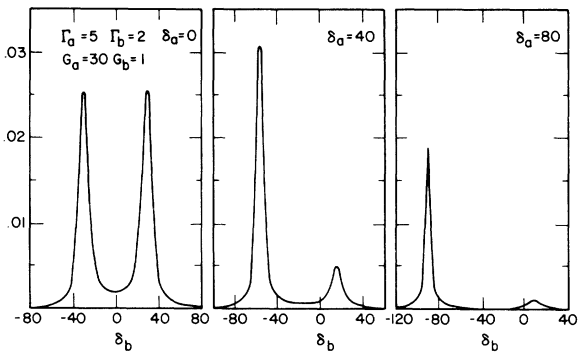

FIG. 5. Absorption spectra showing $\langle\sigma_{33}\rangle$ for a strong lower field and a weak upper field, for three fixed detunings of the lower field.

absorption spectrum there will be a peak near $\delta_a = 0$, even when δ_b is large. As an example, for the same decay constants and field strengths as in Fig. 4, but with δ_b fixed at -800, both $\langle\sigma_{33}\rangle$ and $\langle\sigma_{22}\rangle$ peak at $\delta_a = 800$. These peaks are virtually indistinguishable from those of the third graph of Fig. 4. However, after decreasing to less than 0.002 at $\delta_a \simeq 740$, $\langle\sigma_{22}\rangle$ increases to a maximum of 0.492 at $\delta_a \simeq -1$. The HWHM is 43 for this peak, which exhibits strong power broadening, in contrast to the peak at $\delta_a = 800$. There is also a relative maximum of 0.0007 for $\langle\sigma_{33}\rangle$ at $\delta_a \simeq 2$, and this peak also has a HWHM of about 43. Note that the population of the third atomic state at $\delta_a = 0$ is only $\frac{1}{250}$ of its value at $\delta_a = 800$. We have not presented any graphs of absorption spectra of this second type. However, spectra of either type, for arbitrary values of the parameters, can be plotted from the general solutions given in the Appendix.

Until now we have talked only about the steady-state population distributions, which are reached after the atom has interacted with the applied field for several natural lifetimes. We recall that if a two-level atom interacts with a strong monochromatic field so that $|G| > \Gamma$, then in times short compared to a natural lifetime the populations are oscillating and can reach values considerably different from the steady state. In this regime one talks about optical nutation, π-pulse excitation, and self-induced transparency. The same phenomena can be discussed in the context of a three-level atom interacting with two applied-field modes.

To illustrate the time-dependent behavior of the atom we have chosen an example which shows the importance of the condition that the overall detuning $\delta_a + \delta_b$ equal zero if one wishes to significantly populate the upper excited state. This is, of course, just the condition that the excitation of the atom from state $|1\rangle$ to state $|3\rangle$ with the absorption of one photon from each applied-field mode be energy conserving. Consider an atom whose second and third states have equal decay coefficients of 0.5, and take $|G_a| = |G_b| = 100$, so that the interaction energies are large compared to $\hbar\Gamma_a$ and $\hbar\Gamma_b$. However, they are small compared to the individual detunings, which have been chosen to be $\delta_a = 3000 = -\delta_b$. The atomic-state populations for these values of our parameters are $\langle\sigma_{11}\rangle = 0.338$, $\langle\sigma_{22}\rangle = 0.331$, and $\langle\sigma_{33}\rangle = 0.331$ in the steady state. For short times, however, $\langle\sigma_{11}\rangle$ and $\langle\sigma_{33}\rangle$ oscillate with a period of about $0.94 \times (1/2\Gamma_a)$. Assuming the atom is initially in its ground state, $\langle\sigma_{33}\rangle$ reaches a value of just over 0.80 at the peak of its first oscillation. The value of $\langle\sigma_{11}\rangle$ has fallen to about 0.03 at this same time. This is shown in Fig. 6.

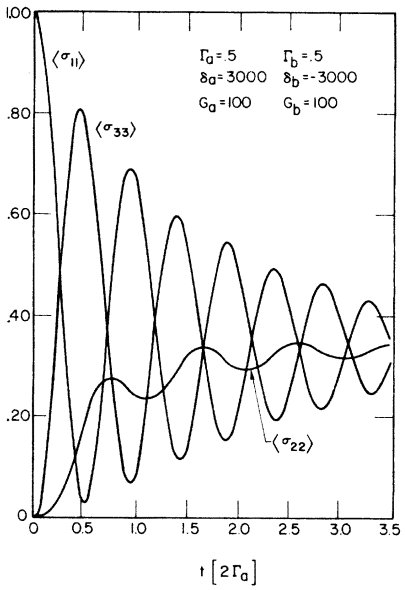

FIG. 6. Transient response of the population distribution during the first few lifetimes after the turn-on of the applied fields.

These very large inversions for short times are more easily obtained for exactly resonant fields. But the fact that they can also be obtained for $|\delta_a| \gg |G|$ when $\delta_a = -\delta_b$ is important. This means, for example, that to excite atoms in a poorly collimated beam by a two-step transition it may not be necessary to saturate the Doppler width. If a suitable middle level can be found so that Ω_a and Ω_b differ only by a few percent, then residual Doppler effects on the overall transition $|1\rangle$ to $|3\rangle$ become negligible when the applied fields propagate in opposite directions. However, to make the periods of oscillation of atoms throughout the Doppler line comparable, the mean detuning δ_a would have to be large compared to the Doppler width. This in turn would require more intense applied fields.

V. SPECTRUM OF SCATTERED LIGHT

With the approximations of Sec. II, the number of photons spontaneously emitted into the mode λ ($\lambda \neq \alpha, \beta$) is given by

$$\langle N(\omega_\lambda, t)\rangle = \left\langle \int_0^t dt' \int_0^t dt'' \left[|g_a^\lambda|^2 \sigma_{21}(t')\sigma_{12}(t'') + |g_b^\lambda|^2 \sigma_{32}(t')\sigma_{23}(t'') \right] \times e^{i\omega_\lambda (t''-t')} \right\rangle . \quad (5.1)$$

The first term on the right-hand side will differ significantly from zero only for those modes λ

whose frequency ω_λ is near ω_a. Similarly, the second term on the right-hand side differs significantly from zero only for those modes λ for which ω_λ is near ω_b. Therefore the number of photons spontaneously emitted with frequency ω_λ near the lower transition frequency is given by

$$\langle N_a(\omega_\lambda, t)\rangle = \left\langle \int_0^t \int_0^t dt'\, dt'' \left| g_a^\lambda \right|^2 \chi_{21}^{(t')} \chi_{12}(t'') \times e^{i(\omega_\lambda - \omega_a)(t''-t')} \right\rangle . \tag{5.2}$$

The number of photons of frequency ω_λ emitted from the upper excited state is given by

$$\langle N_b(\omega_\lambda, t)\rangle = \left\langle \int_0^t \int_0^t dt'\, dt'' \left| g_b^\lambda \right|^2 \chi_{32}(t')\chi_{23}(t'') \times e^{i(\omega_\lambda - \omega_b)(t''-t')} \right\rangle . \tag{5.3}$$

It can be shown[23] that in the long-time limit the correlation functions are stationary in the wide sense, i.e., they then depend only on the time difference t'' - t' as both t' and t'' become large in comparison with the natural lifetimes. In this steady-state limit the spectra become independent of the initial atomic conditions and become proportional to the time derivative of the photon number. From now on we shall consider spectra only in this long-time or steady-state limit. Thus the expressions for the spectra of the light emitted near the upper and lower transition frequencies respectively, simplify to

$$I_a(\omega_\lambda) \propto \lim_{t'\to\infty} \mathrm{Re}\left(\int_0^\infty \langle \chi_{21}(t)\chi_{12}(t+\tau)\rangle e^{i(\omega_\lambda - \omega_a)\tau} d\tau \right), \tag{5.4}$$

$$I_b(\omega_\lambda) \propto \lim_{t'\to\infty} \mathrm{Re}\left(\int_0^\infty \langle \chi_{32}(t)\chi_{23}(t+\tau)\rangle e^{i(\omega_\lambda - \omega_b)\tau} d\tau \right). \tag{5.5}$$

The τ dependence of two-time operators such as $\theta(t', t'') = \chi_{21}(t')\chi_{12}(t'')$, where $t'' = t' + \tau$, is found by taking derivatives with respect to t''. The terms involving a sum over all field modes are eliminated as before by the substitution of a formally integrated solution of the $\dot{c}_\lambda^\dagger$ and $\dot{c}_\lambda$ equations, followed by a harmonic approximation under the integral. The only additional difficulty in simplifying the equations for two-time operators, which was not present for the single-time-operator equations, is commuting $\sigma_{21}(t')$ and $\sigma_{32}(t')$ with $c_\lambda^\dagger(t'')$. This is necessary in order to have the factor $\sum_\lambda c_\lambda^\dagger(0)$ appear on the extreme left-hand side in the operator product, where it simplifies the equations when the expectation value is taken. This commuting introduces no terms into the equations of motion that were not also present in the single-time-operator equations of motion. However, we stress that this is true only because we have $t'' > t'$. When $t'' < t'$, this commutation does introduce additional terms into the equations of motion, which then differ markedly from those for single-time operators. For this reason, a proper understanding of this problem requires a QED calculation, as is discussed in detail elsewhere.[23]

We again assume that the applied fields are described by coherent states. In the spirit of the rotating-wave approximation, we drop those terms which are rapidly oscillating and find a closed set of coupled differential equations with constant coefficients of the form

$$\frac{d}{d\tau} W = A W. \tag{5.6}$$

The matrix A has been given in (3.11). Equation (5.6) has the same form as Eq. (3.10), but with a different interpretation of the variables. The W_i are now expectation values of two-time operators: $W_1(\tau) = \langle \chi_{21}(t')\chi_{33}(t'+\tau)\rangle$, $W_2(\tau) = \langle \chi_{21}(t')\chi_{32}(t'+\tau)\rangle$, etc. for the lower transition; and for the upper transition $W_1'(\tau) = \langle \chi_{32}(t')\chi_{33}(t'+\tau)\rangle$, $W_2'(\tau) = \langle \chi_{32}(t')\chi_{32}(t'+\tau)\rangle$, etc.

Again, a formal solution is easily written down and can be evaluated by computer. The initial conditions are at $\tau = 0$ and t' very large (since we have gone to the stationary limit). Thus the initial conditions involve only the steady-state values of single-time expectation values. The spectrum of light near frequency ω_a is found from

$$I_a(\omega_\lambda) \propto \mathrm{Re} \int_0^\infty W_6(\tau) e^{i(\omega_\lambda - \omega_a)\tau} d\tau , \tag{5.7}$$

and the spectrum near the upper-transition frequency is found from

$$I_b(\omega_\lambda) \propto \mathrm{Re} \int_0^\infty W_8'(\tau) e^{i(\omega_\lambda - \omega_b)\tau} d\tau . \tag{5.8}$$

We have calculated emission spectra for a wide range of values for the parameters. In general, the spectrum associated with each atomic transition frequency may have up to seven separate peaks of greatly varying intensities. Unlike the driven two-level atom, whose emission spectrum is symmetrical about the applied-field frequency, the three-level atom spectra are in general asymmetrical. They become symmetrical only when both applied-field detunings are zero.

Figures 7 and 8 are graphs of the emission spectra in a general case where $\Gamma_a = 1$, $\Gamma_b = 2$, $G_a = 10$, $G_b = 15$, and $\delta_a = 20$. For Fig. 7 we have chosen δ_b to be -20, and for Fig. 8 we have taken $\delta_b = 0$. There is an elastically scattered component in each spectrum that should theoretically be represented as a δ-function at each applied-field

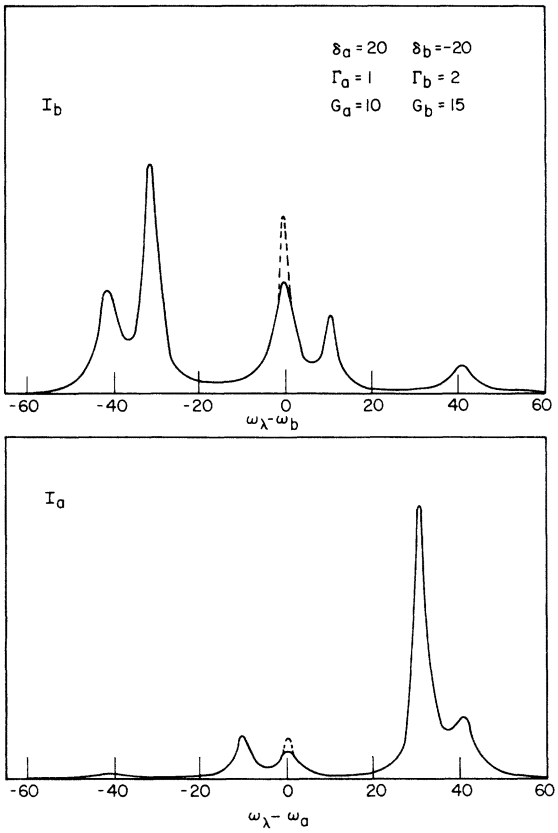

FIG. 7. Emission spectra for a situation where the fields are strong and have opposite detunings.

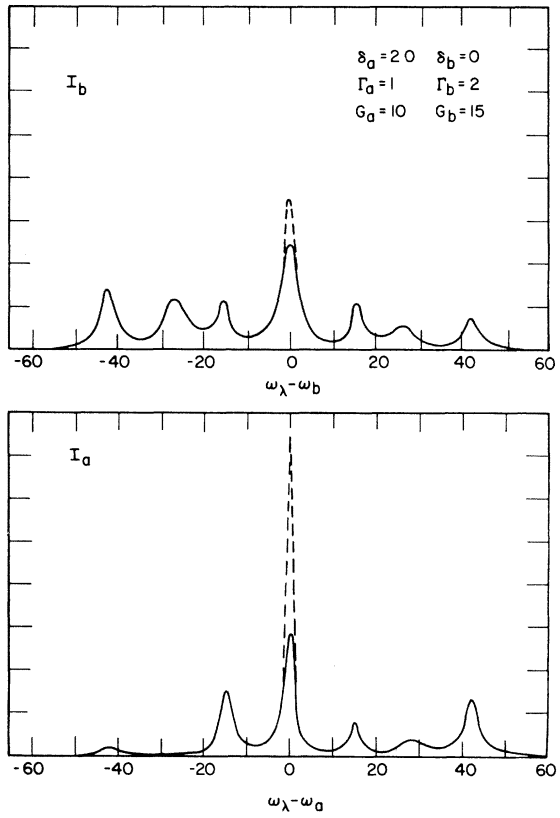

FIG. 8. Emission spectra for the same situation as in Fig. 7, except that the detuning of the field at the upper transition is now zero. Note that all seven peaks near ω_b are of comparable intensity.

frequency. We have represented these in the graphs by Gaussians of the same area with a $1/e$ width of 2, drawn as a broken line.

In Fig. 7 the seven possible peaks occur at $\omega_\lambda - \omega_i = 0$, ± 11, ± 31, and ± 41. In I_a the peaks at -31 and 11 are missing, and the peak at -41 is very small. In I_b the peaks at 31 and -11 are missing. One of the interesting features of these spectra are their skewness about the applied-field frequencies. As a result, the average emitted frequency in I_a is 25 above ω_a, and in I_b the mean frequency is 15.5 below ω_b. Thus the atom is emitting more power near frequency ω_a than it is absorbing at that frequency. This "gain" in energy near ω_a is precisely balanced by a "loss" in energy near frequency ω_b, so that energy is conserved, as expected.

In Fig. 7 each mean emitted frequency was on the atomic frequency side of the applied-field frequency. This effect is more pronounced for greater detunings. For example, for the situation $\Gamma_a = 2$, $\Gamma_b = 0.5$, $G_a = G_b = 20$, and $\delta_a = -\delta_b = 1000$, the average emitted frequencies are 995 above ω_a and 1000 below ω_b. Of course, as the intensity of the second field is lowered, the average frequency emitted in the first transition must move toward ω_a.

In Fig. 8 the second field is exactly resonant with the second transition. I_b is an example of a spectrum in which all seven components are readily visible. The mean frequency of I_a is 7.9 and for I_b is -5.9. Again, energy is conserved for the two transitions considered together.

The mean emitted frequencies are precisely the applied-field frequencies when both detunings are zero. The spectrum in such a situation is shown in Fig. 9 for the values $\Gamma_a = 1$, $\Gamma_b = 3$, $G_a = 20$, and $G_b = 30$. Only five peaks appear because two peaks overlap at the first sideband on each side. The spectra are symmetric about the applied-field frequencies, and the peaks are almost equally spaced. Some interesting properties of these symmetric five-peaked spectra are discussed at the end of Sec. VI.

When both applied fields are below the critical field strengths and near resonance, each spectrum has a single predominant component. For the lower transition most of the light is scattered

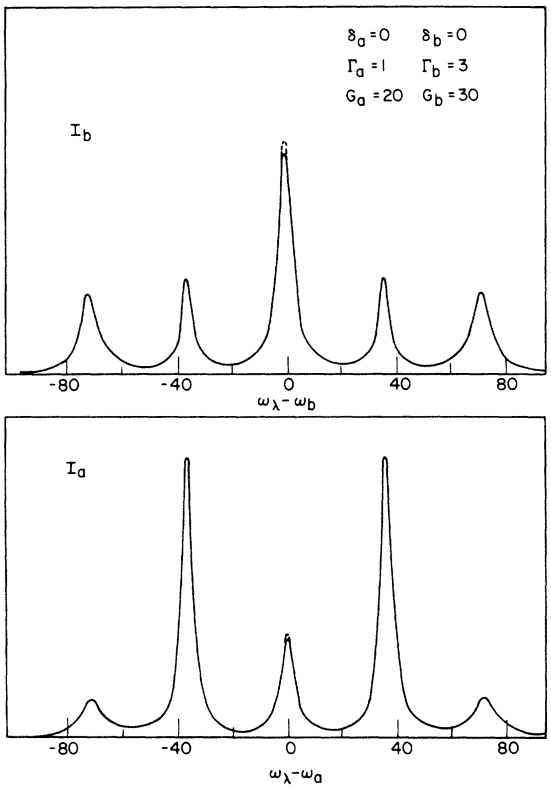

FIG. 9. Emission spectra for a situation with both fields strong and exactly resonant, showing the characteristic five-peaked symmetric shape.

elastically, so the δ-function component is strongest (as in a two-level atom). For the upper transition most of the light is scattered in a line with a HWHM approximately equal to Γ_a, and the intensity of the δ-function component is negligible.

VI. DRESSED STATES AND RATE EQUATIONS

In Sec. IV we commented upon how poorly the usual rate-equation treatment fared in predicting our results. This failure was ascribed to the neglect of the large off-diagonal terms of the density matrix, which were induced by the near-resonant fields. There is an approximation method that does take into account the coherent mixing effects of the applied fields, and which in addition provides a better intuitive understanding of a number of the results of Secs. IV and V than do the complicated and involved formal solutions.

Denote by H_I' only that part of the interaction Hamiltonian H_I of (2.7) which couples the atom to the two initially occupied modes α and β:

$$H_I' = \hbar\left[g_a^{\alpha}\sigma_{21}c_{\alpha} + g_a^{\alpha *}c_{\alpha}^{\dagger}\sigma_{12} + g_b^{\beta}\sigma_{32}c_{\beta} + g_b^{\beta *}c_{\beta}^{\dagger}\sigma_{23}\right]. \tag{6.1}$$

The spectrum of the Hamiltonian $H_A + H_F + H_I'$ is a lattice of closely spaced triplets of eigenstates. Each set of triplets is characterized by a pair of indices (n_a, n_b), which indicates that those triplet states are a linear combination of the three nearly degenerate direct product states $|n_a, n_b\rangle|1\rangle$, $|n_a-1, n_b\rangle|2\rangle$, $|n_a-1, n_b-1\rangle|3\rangle$. The state $|n_a, n_b\rangle$ is a Fock state with n_a photons in the mode α and n_b photons in mode β. These eigenstates are dressed states of the system.[25] The small energy splittings within a triplet are of course due to the coupling of the atom to the applied fields, and are referred to as the resonant Stark effect.

In real laboratory experiments one uses finite-amplitude electromagnetic fields. In a Fock-state description, these are best represented by going to the thermodynamic limit in which the number of photons n_a and n_b in the applied-field modes as well as the field quantization volume V go to infinity in such a way that the photon densities n_a/V and n_b/V approach finite limits. Then the energy splittings will be the same for all triplets within a finite distance of each other on the lattice. Such a lattice of dressed-state triplets is represented in Fig. 10. The vertical dimension represents energy, so this diagram is for $\omega_a < \omega_b$. Subtraction of one photon from mode β, represented by going to the triplet below and to the right-hand side of the original, results in a greater decrease in energy than subtraction of a photon from mode α, represented by going to the triplet below and to the left-hand side of the original.

The part of the Hamiltonian which couples the atom to the infinite number of initially unoccupied modes has so far been ignored. It results in energy being scattered out of the applied fields into the other modes. Such an event can be interpreted as a transition from a dressed state in some triplet

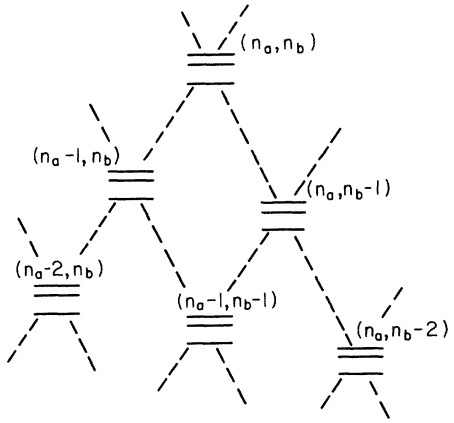

FIG. 10. A representation of the lattice of dressed-state triplets.

into a state of one of the two triplets directly below it (as indicated by the dotted lines in Fig. 10), with the simultaneous emission of a photon of the appropriate frequency. This event is an incoherent process and might be fairly well described by rate equations. Indeed, we have found good agreement between our results in the limit $|G_a|, |G_b| \gg \Gamma_a, \Gamma_b$ and those of a rate-equation calculation on the dressed states. It is only in this strong-field limit, when the decay constants are negligible, that the dressed states (found by neglecting the coupling to the initially unoccupied modes, which gave us Γ_a and Γ_b in Sec. III) are a good first approximation to the eigenstates of the total system.

The asymptotic limits given in Sec. IV for the atomic-state populations were originally found from the following kind of rate-equation calculation on the dressed states. First the dress states $|v_+\rangle$, $|v_0\rangle$, $|v_-\rangle$ were calculated for a particular triplet (n_a, n_b). Then the total decay rate of each state $|v_i\rangle$ to the set of triplets $(n_a - 1, n_b)$ was assumed to be $2\Gamma_a |\langle n_a - 1, n_b; 2|v_i\rangle|^2$; that is, $2\Gamma_a$ times the probability of the atom being in state $|2\rangle$ when the system is in state $|v_i\rangle$. Similarly, the total decay rate of $|v_i\rangle$ to the set of triplets $(n_a, n_b - 1)$ was assumed to be $2\Gamma_b |\langle n_a - 1, n_b - 1; 3|v_i\rangle|^2$. The branching ratios for decay to each state within the triplet $(n_a - 1, n_b)$ were assumed to be given by the probability of the atom being in its ground state $|1\rangle$ when the system was described by that dressed state. The branching ratio to each particular dressed state of the triplet $(n_a, n_b - 1)$ was taken to be the probability of being in atomic state $|2\rangle$ when that dressed state described the system. For example, the decay rate from the state $|v_-\rangle$ in triplet (n_a, n_b) to state $|v_+\rangle$ in triplet $(n_a, n_b - 1)$ is

$$2\Gamma_b |\langle n_a - 1, n_b - 1; 3|v_-\rangle|^2 |\langle n_a - 1, n_b - 1; 2|v_+\rangle|^2 .$$

The cascading down the lattice of dressed states which is given by these rate equations is assumed to describe the process of spontaneous emission. Finally, if one sums over all lattice vertices (i.e., over all occupation numbers for the incident-field modes α and β), one finds that the probabilities of the system being in the upper, middle, or lower state of a triplet soon become independent of time. The corresponding steady-state population distribution for the atomic states can then be easily calculated.

The general rate-equation predictions for exactly resonant fields are

$$\langle \sigma_{11} \rangle = (s^4\Gamma_a + c^4\Gamma_b)/(2c^2\Gamma_b + s^2\Gamma_a), \tag{6.2a}$$

$$\langle \sigma_{22} \rangle = c^2\Gamma_b/(2c^2\Gamma_b + s^2\Gamma_a), \tag{6.2b}$$

$$\langle \sigma_{33} \rangle = s^2c^2(\Gamma_a + \Gamma_b)/(2c^2\Gamma_b + s^2\Gamma_a), \tag{6.2c}$$

where

$$c^2 \equiv |G_a|^2/(|G_a|^2 + |G_b|^2), \tag{6.3}$$

$$s^2 \equiv |G_b|^2/(|G_a|^2 + |G_b|^2). \tag{6.4}$$

These results agree with the solution of Eqs. (3.10) for steady-state populations in the strong-field limit, as can be readily confirmed by comparison with the leading terms of the solutions given in the Appendix.

It is easy to show from Eqs. (6.2) that the steady-state population in the highest atomic state is maximized by the condition

$$c^2/s^2 = (\Gamma_a/2\Gamma_b)^{1/2}. \tag{6.5}$$

Letting $r = (\Gamma_a/2\Gamma_b)^{1/2}$, one finds when this condition is satisfied that

$$\langle \sigma_{33} \rangle_{\max} = (2r^2 + 1)/2(r + 1)^2 . \tag{6.6}$$

As r goes to zero ($\Gamma_a \ll \Gamma_b$), $\langle \sigma_{33} \rangle_{\max}$ approaches $\frac{1}{2}$; as r goes to infinity ($\Gamma_a \gg \Gamma_b$), $\langle \sigma_{33} \rangle_{\max}$ approaches unity. Both of these limits strongly violate the maximum of $\frac{1}{3}$ given by an ordinary rate-equation treatment of the atomic states. The minimum value of (6.6) is exactly $\frac{1}{3}$ and occurs when $\Gamma_b = 2\Gamma_a$.

In the example of Sec. IV where we found $\langle \sigma_{33} \rangle = 0.520$, the system we considered had an r value of 5, which implies an upper limit of 0.5252 on $\langle \sigma_{33} \rangle$. Thus our choice of field strengths there resulted in an upper excited-state population of 99% of the maximum. In a three-level system with $\Gamma_a = 98\Gamma_b$, $\langle \sigma_{33} \rangle_{\max}$ would be about 0.77, corresponding to $r = 7$. Although we know of no strict three-level system with such a disparity in the level decay rates, highly excited states, referred to as Rydberg states,[24] do have very slow rates of decay. Therefore in a transition from the ground state to a first excited state to a Rydberg state it is not difficult to find the ratio of the decay coefficients of the first to the second transition to be 100 or even much greater. Unfortunately, such a high excited state is more likely to decay to a state outside the original three-level system than back to the first excited state.

One can also use this dressed-state rate-equation approach to calculate the integrated intensities of the emission spectrum components. It is obvious by inspection of Fig. 10 that there are nine possible transitions between a pair of triplets. Since three of these transitions are at the applied-field frequency, this means that in general seven peaks will be visible. Also, the three sidebands on either side of the applied-field frequency must be symmetrically placed.

When both applied fields are exactly resonant, the dressed states in the triplet are equally spaced.

Therefore only five components appear in the emission spectrum, and the second sideband will obviously be the same distance from the first sideband as the first sideband is from the central peak. We have made a rate-equation calculation on the dressed states to find the integrated intensities of the emission lines when both detunings are zero. In the lower-transition spectrum, the areas of the peaks are in the ratio

$$\tfrac{1}{2}|G_a|^2 : |G_b|^2 : |G_a|^2 : |G_b|^2 : \tfrac{1}{2}|G_a|^2. \qquad (6.7)$$

For the upper transition the areas under the peaks are in the ratio

$$\tfrac{1}{2}\Gamma_b : \Gamma_a : \Gamma_b : \Gamma_a : \tfrac{1}{2}\Gamma_b. \qquad (6.8)$$

It is interesting that the ratios in the lower transition depend only on the interaction energies, while the ratios in the upper transition only upon the decay constants. Again, these results are expected to be valid only in the strong-field limit. The agreement with the example of Fig. 9 is fairly good. The areas under the smallest peaks in each spectrum are about 10% too large, when the "area under a peak" is defined as the area within adjacent minima of the spectrum. Most of this discrepancy is attributable to the tails of the larger peaks overlapping the smaller peaks. The QED calculation of the area associated with each complex Lorentzian differs by less than 2% from the rate-equation prediction.

VII. SUMMARY

In this paper we have determined the response of a three-level atom irradiated by two near-resonant monochromatic fields. We presented solutions for this model system which are valid over the full range of possible atomic decay constants and incident-field strengths and detunings. Several specific examples of absorption and emission spectra were discussed in detail. The absorption spectra show strong dependence upon the incident-field strengths and detunings. However, if the fields are chosen to equalize the interaction energies of the two transitions, we found that the upper excited-state population peaks at the point of overall resonance ($\delta_a + \delta_b = 0$). Thus for high-resolution spectroscopy one should use strong fields to maximize $\langle\sigma_{33}\rangle$ and hence the signal. But the fixed lower-transition field should be detuned significantly from the middle level to reduce the power broadening and improve the resolution. One can then have an absorption peak for an upper excited state which is narrower than the spontaneous emission line from that state.

The emission spectrum for an atom in the presence of strong fields was shown to consist of seven peaks near each transition frequency. A central peak, which includes a δ-function (i.e., monochromatic) component, appears at the incident-field frequency. Three sidebands appear to each side of this central peak, symmetrically located with respect to it. In spite of this symmetry in the location of these peaks, the spectra are in general asymmetrical, because the intensities of symmetrically placed sidebands are not equal. When both fields are strong and exactly resonant the spectra become symmetrical and have only five peaks.

The lattice of dressed atomic states for the resonant system was discussed, and the usefulness of dressed states in providing an intuitive understanding of a number of our results was stressed. A rate-equation calculation on the dressed states was described which gives results in good quantitative agreement with the exact solutions for strong fields. With it one can easily derive two surprising predictions of the full theory. First, one can show that for certain values of the atomic decay constants the average population in the highest excited state can exceed 50%. Second, in the limit of strong exactly resonant fields, one can show that the ratios of the line intensities for the lower transition depend only upon the interaction energies, and the ratios of the line intensities for the upper transition depend only upon the decay constants.

ACKNOWLEDGMENTS

We thank B. Renaud for many useful discussions and for his critical reading of an earlier version of this paper, and P. Stroud for help in evaluating the expressions found in the Appendix. One of us (R. M. W.) would also like to acknowledge many helpful discussions with R. Kornblith during the beginning stages of this work.

APPENDIX

We found in Sec. IV that the nine quantities $\langle\chi_{ij}\rangle$ became independent of time in the long-time limit [cf. Eq. (4.2)]. Analytic expressions for their steady-state values are derived below.

Consider Eq. (3.10). For large times we may set the derivative equal to zero, which gives us nine linear homogeneous equations in nine unknowns. However, these nine equations, which are of the form

$$A_{i1}V_1 + A_{i2}V_2 + \cdots + A_{i9}V_9 = 0, \quad i = 1, \ldots, 9, \qquad (A1)$$

are not linearly independent. We make a change of variables by dividing each equation by $V_9 = \langle\chi_{22}\rangle$,

and we then neglect the ninth equation ($i=9$). The result is a linearly independent set of eight linear inhomogeneous equations of the form

$$A_{i1}V_1'+\cdots+A_{i8}V_8'+A_{i9}=0, \quad i=1,\ldots,8, \quad \text{(A2)}$$

where

$$V_j'=V_j/V_9. \quad \text{(A3)}$$

This set of equations can be solved by systematically replacing each equation by a linear combination of itself and the other equations. The process is tedious but straightforward. We have derived the following results, where G_a and G_b have been taken to be real:

$$D=G_a^6\Gamma_a\Gamma_b+G_a^4G_b^2\Gamma_b(2\Gamma_a+\Gamma_b)+G_a^2G_b^4\Gamma_b(\Gamma_a+\Gamma_b)+2G_a^4\Gamma_a\Gamma_b\,\mathrm{Re}[(\Gamma_a+\Gamma_b+i\delta_b)(\Gamma_b+i\delta_b+i\delta_a)]$$
$$+G_a^2G_b^2[\Gamma_b^2|\Gamma_a+\Gamma_b+i\delta_b|^2+\Gamma_a(\Gamma_a+\Gamma_b)|\Gamma_b+i\delta_b+i\delta_a|^2]+G_a^2\Gamma_a\Gamma_b|\Gamma_a+\Gamma_b+i\delta_b|^2|\Gamma_b+i\delta_a+i\delta_b|^2, \quad \text{(A4)}$$

$$N_{33}=G_a^4G_b^2\Gamma_a(\Gamma_a+\Gamma_b)+G_a^2G_b^4(\Gamma_a+\Gamma_b)^2+G_a^2G_b^2\Gamma_a\Gamma_b|\Gamma_a+\Gamma_b+i\delta_b|^2, \quad \text{(A5)}$$

$$N_{32}=iG_b\{G_a^4\Gamma_a\Gamma_b(\Gamma_a+\Gamma_b-i\delta_b)+G_a^2G_b^2[\Gamma_b(\Gamma_a+\Gamma_b)(\Gamma_a+\Gamma_b+i\delta_b)+\Gamma_a\Gamma_b(\Gamma_a+\Gamma_b-i\delta_b)-\Gamma_a(\Gamma_a+\Gamma_b)(\Gamma_b-i\delta_b-i\delta_a)]$$
$$+G_a^2\Gamma_a\Gamma_b|\Gamma_a+\Gamma_b+i\delta_b|^2(\Gamma_b+i\delta_b+i\delta_a)\}, \quad \text{(A6)}$$

and

$$\langle\chi_{32}\rangle/\langle\chi_{22}\rangle=N_{32}/D, \quad \text{(A7)}$$

$$\langle\chi_{33}\rangle/\langle\chi_{22}\rangle=N_{33}/D. \quad \text{(A8)}$$

We have found similar expressions for $\langle\chi_{31}\rangle/\langle\chi_{22}\rangle$, $\langle\chi_{21}\rangle/\langle\chi_{22}\rangle$, and $\langle\chi_{11}\rangle/\langle\chi_{22}\rangle$. However, the numerators become progressively more complicated. For numerical evaluation it is preferable to return to the equations themselves and use the fact that the solutions (A7) and (A8) have been found. One then has

$$\frac{\langle\chi_{31}\rangle}{\langle\chi_{22}\rangle}=\left(\frac{G_b}{G_a}-\frac{G_b}{G_a}\frac{\langle\chi_{33}\rangle}{\langle\chi_{22}\rangle}+\frac{(\Gamma_a+\Gamma_b-i\delta_a)}{iG_a}\frac{\langle\chi_{32}\rangle}{\langle\chi_{22}\rangle}\right), \quad \text{(A9)}$$

$$\frac{\langle\chi_{21}\rangle}{\langle\chi_{22}\rangle}=\frac{1}{G_b}\left(G_a\frac{\langle\chi_{33}\rangle}{\langle\chi_{22}\rangle}-i(\Gamma_b-i\delta_b-i\delta_a)\frac{\langle\chi_{31}\rangle}{\langle\chi_{22}\rangle}\right), \quad \text{(A10)}$$

$$\frac{\langle\chi_{11}\rangle}{\langle\chi_{22}\rangle}=\left(1-\frac{G_b}{G_a}\frac{\langle\chi_{31}\rangle}{\langle\chi_{22}\rangle}-\frac{i(\Gamma_a-i\delta_a)}{G_a}\frac{\langle\chi_{21}\rangle}{\langle\chi_{22}\rangle}\right). \quad \text{(A11)}$$

The individual expectation values can now be found by using the conservation-of-population relation (3.9), along with (A7) and (A11), to find $\langle\chi_{22}\rangle$.

The solutions above are exact and can be readily programmed to provide absorption spectra as a function of δ_a or δ_b, for example. Also, for zero detunings and strong fields ($G_a, G_b \gg \Gamma_a, \Gamma_b$) the leading terms in the ratio $\langle\chi_{33}\rangle/\langle\chi_{22}\rangle$, as given by (A7), are seen to be in agreement with the results (6.2b) and (6.2c) found from a rate-equation analysis on the dressed states.

*Work supported in part by the Office of Naval Research through Contract No. N0014-68-A-0091.

[1]I. I. Agarbiceanu and I. M. Popescu, *Optical Methods of Radio Frequency Spectroscopy* (Wiley, New York, 1975) [translated from *Metode Optice Ale Spectroscopiei Hertziene*, (Editura Academiei Republicii Socialiste Romania, Bucharest, 1970)].

[2]R. L. Berger, J. B. West, and T. L. English, Appl. Phys. Lett. 27, 31 (1975).

[3]J. E. Bjorkholm and P. F. Liao, Phys. Liao, Phys. Rev. Lett. 33, 128 (1974); P. F. Liao and J. E. Bjorkholm, *ibid.* 34, 1 (1975).

[4]D. L. Rousseau and P. F. Williams, Phys. Rev. Lett. 33, 1368 (1974).

[5]H. T. Duong, S. Liberman, J. Pinard, and J. L. Vialle, Phys. Rev. Lett. 33, 339 (1974); W. Hartig, V. Wiekl, and H. Walther, Opt. Commun. 14, 244 (1975).

[6]N. Tan-no, K. Yokoto, and H. Inaba, Phys. Rev. Lett. 29, 1211 (1972).

[7]F. Schuda, C. R. Stroud, Jr., and M. Hercher, J. Phys. B 7, L198 (1974); H. Walther, in *Laser Spectroscopy*, edited by S. Haroche, J. C. Pebay-Peyroula, T. W. Hänsch, and S. E. Harris (Springer, New York, 1975), p. 358; F. Y. Wu, R. E. Grove, and S. Ezekiel, Phys. Rev. Lett. 35, 1426 (1975).

[8]M. S. Feld and A. Javan, Phys. Rev. 177, 540 (1969).

[9]T. Hänsch and P. Toschek, Z. Phys. 236, 213 (1970).

[10]B. J. Feldman and M. S. Feld, Phys. Rev. A 5, 899 (1972).

[11]I. M. Beterov and V. P. Chebotaev, *Progress in Quantum Electronics*, edited by J. H. Sanders and S. Stenholm (Pergamon, Oxford, 1974), Vol. 3, Pt. 1.

[12]W. R. Bennett, Jr., Phys. Rev. 126, 580 (1962).

[13]W. E. Lamb, Jr., Phys. Rev. 134, A1420 (1964).

[14]R. G. Brewer and E. L. Hahn, Phys. Rev. A 11, 1641 (1975).

[15]R. Salomaa and S. Stenholm, J. Phys. B 8, 1795 (1975).

[16]D. Grischkowsky and M. M. T. Loy, Phys. Rev. A 12, 1117 (1975).

[17]J. R. Ackerhalt and J. H. Eberly, Phys. Rev. D 10, 3350 (1974).

[18]I. R. Senitzky, Phys. Rev. Lett. 31, 955 (1973); P. W. Milonni, J. R. Ackerhalt, and W. A. Smith, *ibid.* 31, 958 (1973); P. W. Milonni and W. A. Smith, Phys. Rev.

A 11, 814 (1975).
[19]J. R. Ackerhalt, P. L. Knight, and J. H. Eberly, Phys. Rev. Lett. 30, 456 (1973).
[20]Terms involving these generalized decay constants have usually been neglected, as they are in this paper. However, they do enter naturally in QED theory, and their neglect can cause a noticeable error in the calculated emission spectrum in some situations. A discussion and specific examples are given by B. Renaud, Ph.D. thesis (University of Rochester, 1976) (unpublished).
[21]F. Schuda, Ph.D. thesis (University of Rochester, 1974) (unpublished).
[22]C. R. Stroud, Jr., Phys. Rev. A 3, 1044 (1971); E. T. Jaynes and F. W. Cummings, Proc. IEEE 51, 89 (1963).
[23]B. Renaud, R. M. Whitley, and C. R. Stroud, Jr., J. Phys. B 9, L19 (1976).
[24]A brief review of recent interest in highly excited atoms is given in Phys. Today 28, No. 11, 17 (1975).
[25]For an extensive discussion of dressed states, see S. Haroche, Ann. Phys. (Paris) 6, 189 (1971); 6, 327 (1971), and references therein.